CONFERENCE SERIES

Hans-Peter Schröcker, Manfred Husty (eds.)

Proceedings of the 16th International Conference on Geometry and Graphics

Innsbruck, August 4-8, 2014

innsbruck university press

A STUDY ON SPATIAL CYCLOID GEARING

Giorgio FIGLIOLINI[1], Hellmuth STACHEL[2], and Jorge ANGELES[3]
[1]University of Cassino & Southern Lazio, Italy [2]Vienna University of Technology, Austria
[3]McGill University, Montréal, Canada

ABSTRACT: Understanding the geometry of gears with skew axes is a complex task, hard to grasp and to visualize. However, due to Study's Principle of Transference, the geometric treatment based on dual vectors can be readily derived from that of the spherical case. This paper is based on Martin Disteli's work and on the authors' previous results where Camus' concept of an auxiliary curve is extended to the case of skew gears. We focus on the spatial analogue of the following case of cycloid bevel gears: When the auxiliary curve is specified as a pole tangent, we obtain 'pathologic' spherical involute gears with vanishing pressure angle. The profiles are always penetrating at the meshing point because of G^2-contact.
In view of the Camus Theorem, the spatial analogue of the pole tangent is a skew orthogonal helicoid Π_4 as auxiliary surface. Its axis lies on the cylindroid and is normal to the instant screw axis (ISA). Under the roll-sliding of Π_4 along the axodes Π_2 and Π_3 of the gears, any generator g of Π_4 traces a pair of conjugate flanks Φ_2, Φ_3 with permanent line contact. Again, these flanks are not realizable because of the reasons below:
(1) When g coincides with the ISA, the singular lines of the two flanks come together. At each point of g the two flanks share the tangent plane, but in the case of external gears the surfaces open toward opposite sides.
(2) We face the spatial analogue of a spherical G^2-contact, which surprisingly does not mean a G^2-contact at all points of g but only at a single point combined with a mutual penetration of the flanks Φ_2 and Φ_3.
However, when instead of a line g a plane Φ_4 is attached to the right helicoid Π_4, the envelopes of Φ_4 under the roll-sliding of Π_4 along Π_2 and Π_3 are torses that serve as conjugate tooth flanks Φ_2, Φ_3 with a permanent line contact. So far, it seems that these flanks, Φ_2 and Φ_3, are geometrically feasible. This is a possible spatial generalization of octoidal gears or even of planar involute gears.

Keywords: Gears with skew axes, Cycloidal gearing, Involute gearing, Cylindroid, Camus Theorem

1. INTRODUCTION

Let the motions of two gears Σ_2, Σ_3, against the gear box Σ_1 be given, i.e., the rotations Σ_2/Σ_1, Σ_3/Σ_1 about fixed skew axes p_{21} and p_{31} with angular velocities ω_{21}, ω_{31}, respectively. The dual unit vectors representing the axes p_{21} and p_{31} are denoted by $\widehat{\mathbf{p}}_{21}$ and $\widehat{\mathbf{p}}_{31}$, respectively. We use a Cartesian coordinate frame $\mathscr{F}(O;x_1,x_2,x_3)$ with $\widehat{\mathbf{e}}_1, \widehat{\mathbf{e}}_2$ denoting the dual unit vectors of the x_1- and x_2-axis. The given axes p_{21} and p_{31} of the wheels are assumed to be symmetrically placed with respect to the x_1-axis such that the x_3-axis is the common normal of the gear axes.

Using the *dual angle* $\widehat{\alpha} = \alpha + \varepsilon\alpha_0$ between the x_1-axis and p_{21}, we can set (see Fig. 1)

$$\begin{aligned} \widehat{\mathbf{p}}_{21} &= \cos\widehat{\alpha}\,\widehat{\mathbf{e}}_1 - \sin\widehat{\alpha}\,\widehat{\mathbf{e}}_2, \\ \widehat{\mathbf{p}}_{31} &= \cos\widehat{\alpha}\,\widehat{\mathbf{e}}_1 + \sin\widehat{\alpha}\,\widehat{\mathbf{e}}_2. \end{aligned} \tag{1}$$

We limit ourselves to the skew case and assume

$$0 < \alpha < \pi/2 \text{ and } \alpha_0 \neq 0 \tag{2}$$

though most of the arguments hold also in the spherical case, $\alpha_0 = 0$, and in the planar case, $\alpha = 0$, with parallel axes.

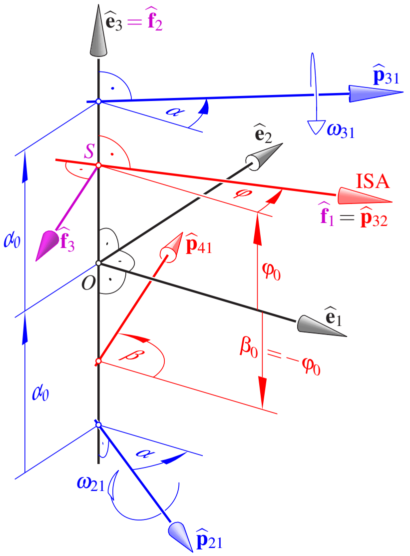

Figure 1: Skew axes $\widehat{\mathbf{p}}_{21}$, $\widehat{\mathbf{p}}_{31}$ of the gear wheels, the ISA $\widehat{\mathbf{p}}_{32}$ and the axis $\widehat{\mathbf{p}}_{41}$ of the auxiliary surface $\Pi_4 \subset \Sigma_4$ in the particular case $\beta = \varphi + \pi/2$. The oriented lines $\widehat{\mathbf{f}}_1, \widehat{\mathbf{f}}_2, \widehat{\mathbf{f}}_3$ form the Frenet frame of the axodes. This frame remains fixed in the gear frame Σ_1.

In addition, let $\widehat{\varphi}$ denote the dual angle between $\widehat{\mathbf{e}}_1$ and the ISA, i.e., the relative axis $\widehat{\mathbf{p}}_{32}$. Then we obtain

$$\begin{aligned} \widehat{\mathbf{p}}_{32} &= \cos\widehat{\varphi}\,\widehat{\mathbf{e}}_1 + \sin\widehat{\varphi}\,\widehat{\mathbf{e}}_2 \ \text{ and} \\ \widehat{\omega}_{32}\,\widehat{\mathbf{p}}_{32} &= \omega_{31}\,\widehat{\mathbf{p}}_{31} - \omega_{21}\,\widehat{\mathbf{p}}_{21}. \end{aligned} \tag{3}$$

The comparison of coefficients and [4, Eq. (7)] lead to

$$\begin{aligned} \tan\varphi &= \frac{\omega_{31} + \omega_{21}}{\omega_{31} - \omega_{21}} \tan\alpha \ \text{ and} \\ \varphi_0 &= R\sin 2\varphi \ \text{ with } R = \frac{\alpha_0}{\sin 2\alpha}. \end{aligned} \tag{4}$$

The vector product of both sides of the last equation in (3) with $\widehat{\mathbf{p}}_{21}$ and $\widehat{\mathbf{p}}_{31}$ (compare [6, Eq. (12)]) results in

$$\frac{\omega_{21}}{\sin(\widehat{\varphi} - \widehat{\alpha})} = \frac{\omega_{31}}{\sin(\widehat{\varphi} + \widehat{\alpha})} = \frac{\widehat{\omega}_{32}}{\sin 2\widehat{\alpha}}, \tag{5}$$

which sometimes is called the *dual Sine-Theorem* applied to the dual 'triangle' $\omega_{21}\,\widehat{\mathbf{p}}_{21}$ and $\omega_{31}\,\widehat{\mathbf{p}}_{31}$ and $\widehat{\omega}_{32}\,\widehat{\mathbf{p}}_{32}$. This implies

$$\widehat{\omega}_{32} = \frac{\omega_{21}\sin 2\widehat{\alpha}}{\sin(\widehat{\varphi} - \widehat{\alpha})} \tag{6}$$

and, consequently, for the pitch of the relative motion Σ_3/Σ_2 like [4, Eq. (15)]

$$\begin{aligned} h_{32} &= \frac{\omega_{320}}{\omega_{32}} = R(\cos 2\alpha - \cos 2\varphi) \\ &= 2R(\cos^2\alpha - \cos^2\varphi). \end{aligned} \tag{7}$$

The axodes of the relative motion Σ_3/Σ_2 are one-sheet hyperboloids $\Pi_3 \subset \Sigma_3$ and $\Pi_2 \subset \Sigma_2$, swept by the relative axis p_{32} under the inverse rotations Σ_1/Σ_2 and Σ_1/Σ_3 about p_{21} and p_{31}, respectively.

2. THE SPATIAL CAMUS THEOREM

The following lemma was first published by Disteli (see [6, Theorem 2] and the references therein).

Lemma 1. *For given wheels Σ_2, Σ_3 there exists a frame Σ_4 such that the screws of Σ_4/Σ_2, Σ_4/Σ_3 and Σ_3/Σ_2 are equal at every instant if and only if the instant axis p_{41} of Σ_4/Σ_1 is located on the Plücker conoid Ψ, but different from p_{32}.*

Let $\widehat{\beta}$ be the dual angle between between the x_1-axis and $\widehat{\mathbf{p}}_{41}$ (Fig. 1). Then we can write

$$\widehat{\mathbf{p}}_{41} = \cos\widehat{\beta}\,\widehat{\mathbf{e}}_1 + \sin\widehat{\beta}\,\widehat{\mathbf{e}}_2. \tag{8}$$

If we specify $p_{41} \subset \Psi$ different from p_{21}, p_{31}, p_{32}, then $\varphi \neq \pm\alpha, \beta$. From the equation [6, Eq. (8)], which defines the Plücker conoid, we obtain

$$\beta_0 = R\sin 2\beta. \tag{9}$$

The dual Sine-Theorem applied to the triangle $\omega_{21}\,\widehat{\mathbf{p}}_{21}$, $\widehat{\omega}_{41}\,\widehat{\mathbf{p}}_{41}$ and $\widehat{\omega}_{42}\,\widehat{\mathbf{p}}_{42} = \widehat{\omega}_{42}\,\widehat{\mathbf{p}}_{32}$ gives (compare [6, Eq. (12)])

$$\frac{\omega_{21}}{\sin(\widehat{\varphi} - \widehat{\beta})} = \frac{\widehat{\omega}_{41}}{\sin(\widehat{\varphi} + \widehat{\alpha})} = \frac{\widehat{\omega}_{42}}{\sin(\widehat{\alpha} + \widehat{\beta})} \tag{10}$$

and, analogously, for $\omega_{31}\,\widehat{\mathbf{p}}_{31}$, $\widehat{\omega}_{41}\,\widehat{\mathbf{p}}_{41}$ and $\widehat{\omega}_{43}\,\widehat{\mathbf{p}}_{43} = \widehat{\omega}_{43}\,\widehat{\mathbf{p}}_{32}$

$$\frac{\omega_{31}}{\sin(\widehat{\varphi}-\widehat{\beta})} = \frac{\widehat{\omega}_{41}}{\sin(\widehat{\varphi}-\widehat{\alpha})} = \frac{\widehat{\omega}_{43}}{\sin(\widehat{\beta}-\widehat{\alpha})}. \tag{11}$$

The instant pitch $h_{41} = \omega_{410}/\omega_{41}$ is defined by [6, Eq. (9)] as

$$h_{41} = \frac{\omega_{410}}{\omega_{41}} = R(\cos 2\alpha - \cos 2\beta). \tag{12}$$

Let Π_4 be the ruled helical surface[1] traced by the relative axis p_{32} under the helical motion Σ_1/Σ_4 about p_{41} with pitch h_{41}. We call Π_4 the *auxiliary surface* (for further details see [5]). It forms together with Π_2 and Π_3 the axodes of the relative motions of Σ_4 against Σ_2 and Σ_3, i.e., the motions Σ_4/Σ_2 and Σ_4/Σ_3 are defined by the rolling and sliding of Π_4 along the hyperboloids Π_2 and Π_3, respectively.

The importance of the auxiliary surface $\Pi_4 \subset \Sigma_4$ lies in [6, Theorem 3] which we recall as below:

Theorem 2. [Spatial Camus Theorem]
For any line g attached to Σ_4, the surfaces Φ_2, Φ_3 traced by g under the relative motions Σ_4/Σ_2 and Σ_4/Σ_3, respectively, are conjugate tooth flanks of Σ_3/Σ_2. At any instant, the meshing points for these flanks are located on a straight line.

With respect to the gear frame Σ_1, the locus of the meshing lines, i.e., the *meshing surface* or *surface of action*, is traced by g under Σ_4/Σ_1 with the fixed twist $\widehat{\mathbf{q}}_{41} = \widehat{\omega}_{41}\,\widehat{\mathbf{p}}_{41}$. Consequently, it is a helical surface with axis $\widehat{\mathbf{p}}_{41}$.

3. THE DISTELI AXES OF A RULED SURFACE

Along each non-torsal generator g of a ruled surface a *Frenet frame* can be defined, consisting of: g itself; the *central normal* n, which is the surface normal at the striction point; and the *central tangent* t (see, e.g., [1, 2]). This triplet of mutually orthogonal axes meets at the *striction point* S of g, defined on the *striction curve* (Fig. 2). The central tangent is orthogonal to the asymptotic plane and tangent to the surface at the striction point.

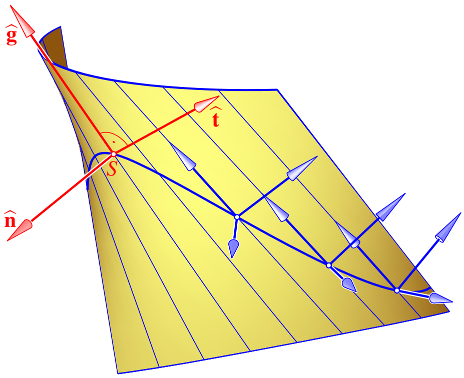

Figure 2: Frenet frame $(\widehat{\mathbf{g}}, \widehat{\mathbf{n}}, \widehat{\mathbf{t}})$ and striction curve of a ruled surface.

Let, in dual-vector notation[2], the ruled surface be given by the twice-differentiable dual vector function $\widehat{\mathbf{g}}(t)$, $t \in I$. Then, the derivatives of the Frenet frame $(\widehat{\mathbf{g}}, \widehat{\mathbf{n}}, \widehat{\mathbf{t}})$ satisfy the *Frenet equations*—Eq. (10) of [1]—namely,

$$\begin{aligned} \dot{\widehat{\mathbf{g}}} &= \qquad \widehat{\lambda}\,\widehat{\mathbf{n}} \qquad &= \widehat{\mathbf{q}}\times\widehat{\mathbf{g}} \\ \dot{\widehat{\mathbf{n}}} &= -\widehat{\lambda}\,\widehat{\mathbf{g}} \qquad +\widehat{\mu}\,\widehat{\mathbf{t}} &= \widehat{\mathbf{q}}\times\widehat{\mathbf{n}} \\ \dot{\widehat{\mathbf{t}}} &= \qquad -\widehat{\mu}\,\widehat{\mathbf{n}}. \qquad &= \widehat{\mathbf{q}}\times\widehat{\mathbf{t}} \end{aligned} \tag{13}$$
$$\text{with } \widehat{\mathbf{q}} = \widehat{\mu}\,\widehat{\mathbf{g}} + \widehat{\lambda}\,\widehat{\mathbf{t}} = \widehat{\omega}\,\widehat{\mathbf{g}}^*,$$

$\widehat{\mathbf{g}}^*$ with $\widehat{\mathbf{g}}^*\cdot\widehat{\mathbf{g}}^* = 1$ being the *Disteli axis* and $\widehat{\omega}^2 = \widehat{\lambda}^2 + \widehat{\mu}^2$, provided $\widehat{\lambda} \neq 0$. By the last condition we exclude stationary (= singular) generators.

The Frenet equations (13) contain two dual coefficients, $\widehat{\lambda} = \lambda + \varepsilon\lambda_0$ and $\widehat{\mu} = \mu + \varepsilon\mu_0$. Various formulas expressing invariants of the ruled

[1] In this paper the term 'ruled surface' stands for a twice continuously differentiable one-parameter set of oriented lines.

[2] From now on we identify oriented lines with their dual unit vector—with respect to any well-defined coordinate frame. In this sense we speak of the 'line $\widehat{\mathbf{g}}$'.

surface in terms of λ, λ_0, μ, and μ_0 can be found in [1, Theorems 1–3].[3] Here we adopt a different approach.

The dual representation $\widehat{\mathbf{g}}(t) = \mathbf{g}(t) + \varepsilon\,\mathbf{g}_0(t)$, $t \in I$, of the ruled surface gives rise to a real parametrization, namely

$$\mathbf{x}(t,u) = [\mathbf{g}(t) \times \mathbf{g}_0(t)] + u\,\mathbf{g}(t), \quad (t,u) \in I \times \mathbb{R}. \tag{14}$$

Here we recall that $\mathbf{g} \times \mathbf{g}_0$ is the position vector of the pedal point of the generator $\widehat{\mathbf{g}}$ with respect to the origin of the underlying coordinate frame. The derivatives

$$\begin{aligned}
\frac{d}{dt}\widehat{\mathbf{g}} &= \dot{\widehat{\mathbf{g}}} = \dot{\mathbf{g}} + \varepsilon\dot{\mathbf{g}}_0 = \widehat{\lambda}\,\widehat{\mathbf{n}} \\
&= \lambda\mathbf{n} + \varepsilon\,(\lambda_0\mathbf{n} + \lambda\mathbf{n}_0)\,, \\
\frac{d^2}{dt^2}\widehat{\mathbf{g}} &= \ddot{\widehat{\mathbf{g}}} = \ddot{\mathbf{g}} + \varepsilon\ddot{\mathbf{g}}_0 = -\widehat{\lambda}^2\widehat{\mathbf{g}} + \dot{\widehat{\lambda}}\,\widehat{\mathbf{n}} + \widehat{\lambda}\,\widehat{\mu}\,\widehat{\mathbf{t}} \\
&= -\lambda^2\mathbf{g} + \dot{\lambda}\mathbf{n} + \lambda\mu\mathbf{t} + \varepsilon\big(-2\lambda\lambda_0\mathbf{g} - \lambda^2\mathbf{g}_0 \\
&\qquad + \dot{\lambda}_0\mathbf{n} + \dot{\lambda}\mathbf{n}_0 + \lambda_0\mu\mathbf{t} + \lambda\mu_0\mathbf{t} + \lambda\mu\mathbf{t}_0\big)
\end{aligned} \tag{15}$$

determine the partial derivatives of the parametrization $\mathbf{x}(t,u)$:

$$\mathbf{x}_t = (\dot{\mathbf{g}} \times \mathbf{g}_0) + (\mathbf{g} \times \dot{\mathbf{g}}_0) + u\dot{\mathbf{g}}, \quad \mathbf{x}_u = \mathbf{g}$$

and

$$\begin{gathered}
\mathbf{x}_{tt} = (\ddot{\mathbf{g}} \times \mathbf{g}_0) + 2(\dot{\mathbf{g}} \times \dot{\mathbf{g}}_0) + (\mathbf{g} \times \ddot{\mathbf{g}}_0) + u\ddot{\mathbf{g}}, \\
\mathbf{x}_{tu} = \dot{\mathbf{g}} = \lambda\mathbf{n}, \quad \mathbf{x}_{uu} = \mathbf{0}.
\end{gathered}$$

We study the derivatives at the points of a single generator, say, at $t = 0$. For this purpose we use the triplet $\big(\widehat{\mathbf{g}}(0), \widehat{\mathbf{n}}(0), \widehat{\mathbf{t}}(0)\big)$ as the new coordinate frame; now the striction point $\mathbf{s}(0)$ of $\widehat{\mathbf{g}}(0)$ is the origin of the frame in question. Thus we may set

$$\mathbf{g}(0) = \begin{pmatrix}1\\0\\0\end{pmatrix}, \ \mathbf{n}(0) = \begin{pmatrix}0\\1\\0\end{pmatrix}, \ \mathbf{t}(0) = \begin{pmatrix}0\\0\\1\end{pmatrix},$$
$$\mathbf{g}_0(0) = \mathbf{n}_0(0) = \mathbf{t}_0(0) = \mathbf{0}.$$

This yields

$$\dot{\widehat{\mathbf{g}}}(0) = \begin{pmatrix}0\\\lambda\\0\end{pmatrix} + \varepsilon\begin{pmatrix}0\\\lambda_0\\0\end{pmatrix},$$

$$\ddot{\widehat{\mathbf{g}}}(0) = \begin{pmatrix}-\lambda^2\\\dot{\lambda}\\\lambda\mu\end{pmatrix} + \varepsilon\begin{pmatrix}-2\lambda\lambda_0\\\dot{\lambda}_0\\\lambda_0\mu + \lambda\mu_0\end{pmatrix}$$

and therefore

$$\mathbf{x}_t(0,u) = \begin{pmatrix}0\\\lambda u\\\lambda_0\end{pmatrix}, \quad \mathbf{x}_u(0,u) = \begin{pmatrix}1\\0\\0\end{pmatrix}, \tag{16}$$

$$\begin{gathered}
\mathbf{x}_{tt}(0,u) = \begin{pmatrix}-\lambda^2 u\\-\lambda_0\mu - \lambda\mu_0 + \dot{\lambda}u\\\dot{\lambda}_0 + \lambda\mu u\end{pmatrix}, \\
\mathbf{x}_{tu}(0,u) = \begin{pmatrix}0\\\lambda\\0\end{pmatrix}, \ \mathbf{x}_{uu}(0,u) = \begin{pmatrix}0\\0\\0\end{pmatrix}.
\end{gathered} \tag{17}$$

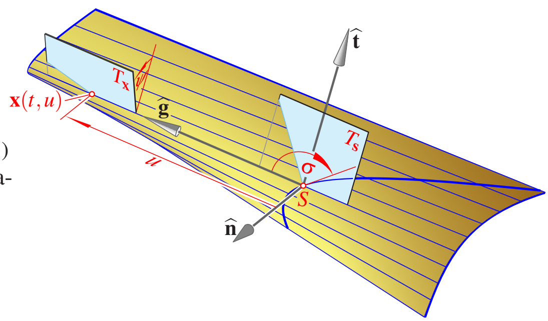

Figure 3: The distribution parameter δ defines the tangent planes $T_{\mathbf{x}}$ along the generator $\widehat{\mathbf{g}}$ by $\tan\psi = -u/\delta$. The angle σ between $\widehat{\mathbf{g}}$ and the striction curve is called the *striction angle* or the *striction*.

The vector product $\mathbf{b} = \mathbf{x}_t \times \mathbf{x}_u$ is a normal vector of the ruled surface, provided the surface point is regular, which means $\mathbf{b} \neq \mathbf{0}$. The coordinates

$$\mathbf{b}(0,u) = \begin{pmatrix}0\\\lambda_0\\-\lambda u\end{pmatrix} \tag{18}$$

reveal that at generators with $\lambda\lambda_0 \neq 0$ the angle ψ between the central normal vector $\mathbf{b}(0,0) = \lambda\mathbf{n}$ and the normal vector $\mathbf{b}(0,u)$ (see Fig. 3) satisfies the equation

$$\tan\psi = \frac{-\lambda u}{\lambda_0} = -\frac{u}{\delta} \quad \text{with} \quad \delta = \frac{\lambda_0}{\lambda}. \tag{19}$$

[3]For example: The dual part $\mathbf{q}_0$ of the twist $\widehat{\mathbf{q}}$ equals the instant velocity vector of the origin $\mathbf{s}$. Consequently, for the striction σ (see Fig. 3) we get $\tan\sigma = \lambda/\mu$.

The quotient δ is called the *distribution parameter*. This is a geometric invariant, i.e., invariant against parameter transformations. Generators with $\lambda_0 = 0$ and hence $\delta = 0$ are called *torsal*: Here all points with $u \neq 0$ have the same tangent plane; the striction point $(u = 0)$ is singular because of $\mathbf{b}(0,0) = \mathbf{0}$.

Cylindrical generators are defined by $\dot{\mathbf{g}} = \mathbf{0}$ or $\lambda = 0$. Here, all points are possible striction points, for which we set $\delta := \infty$.

4. TWO RULED SURFACES WITH LINE CONTACT

For our study on cycloid gearing we need some results concerning the Disteli axes $\widehat{\mathbf{g}}^*$ of a ruled surface. According to (13), $\widehat{\mathbf{q}} = \widehat{\omega}\widehat{\mathbf{g}}^*$ is the twist and therefore $\widehat{\mathbf{g}}^*$ the instant screw axis of the moving Frenet frame. From Eqs. (15) and (13) follows the relation below:

$$\begin{aligned} \dot{\widehat{\mathbf{g}}} \times \ddot{\widehat{\mathbf{g}}} &= \widehat{\lambda}\,\widehat{\mathbf{n}} \times (-\widehat{\lambda}^2\widehat{\mathbf{g}} + \dot{\widehat{\lambda}}\,\widehat{\mathbf{n}} + \widehat{\lambda}\,\widehat{\mu}\,\widehat{\mathbf{t}}) \\ &= \widehat{\lambda}^2\,\widehat{\omega}\,\widehat{\mathbf{g}}^*. \end{aligned} \tag{20}$$

Due to [1, Theorem 3, 3], the dual angle $\widehat{\gamma} = \gamma + \varepsilon\gamma_0$ between the generator $\widehat{\mathbf{g}}$ and the corresponding Disteli axis $\widehat{\mathbf{g}}^*$ satisfies

$$\begin{aligned} \cot\widehat{\gamma} &= \frac{\widehat{\mu}}{\widehat{\lambda}}, \text{ hence} \\ \cot\gamma = \frac{\mu}{\lambda} &\text{ and } \gamma_0 = \frac{\lambda\mu_0 - \lambda_0\mu}{\lambda^2 + \mu^2}. \end{aligned} \tag{21}$$

This is a consequence of the two standard products

$$\widehat{\mathbf{g}} \cdot \widehat{\mathbf{g}}^* = \cos\widehat{\gamma} = \frac{\widehat{\mu}}{\widehat{\omega}}, \quad \widehat{\mathbf{g}} \times \widehat{\mathbf{g}}^* = \sin\widehat{\gamma}\widehat{\mathbf{n}} = -\frac{\widehat{\lambda}}{\widehat{\omega}}\,\widehat{\mathbf{n}},$$

and of the rule that the dual extension of an analytic real function $f(t)$ is defined as $f(\widehat{t}) = f(t + \varepsilon t_0) = f(t) + \varepsilon t_0 \dot{f}(t)$, which yields

$$\cot\widehat{\gamma} = \cot\gamma + \varepsilon\gamma_0(1 + \cot^2\gamma).$$

The dual angle between the moving $\widehat{\mathbf{g}}(t)$ and the fixed $\widehat{\mathbf{g}}^*(0)$ is stationary of order 2 at $t = 0$ (see [1, Theorem 3, 4]). Due to the spherical analogy, $\cot\widehat{\gamma}$ can be called the *dual (geodesic) curvature* of the ruled surface.

Lemma 3. *If two ruled surfaces are in contact at all points of a common generator and if they share the corresponding Frenet frame and the Disteli axis, then their dual coefficients in the Frenet equations differ at the corresponding parameter values only by a real factor $c \neq 0$.*

The proof is straightforward and left for the reader.

Theorem 4. *Let $\widehat{\mathbf{g}}(t)$ and $\widetilde{\widehat{\mathbf{g}}}(\widetilde{t})$ be two twice-differentiable ruled surfaces which at $t = \widetilde{t} = 0$ share the Frenet frame, the distribution parameter $\delta(0) = \tilde{\delta}(0)$ and the Disteli axis. Then, the surfaces have a G^2-contact at the striction point of the common generator.*

If by Lemma 3 $\widetilde{\widehat{\lambda}}(0) = c\,\widehat{\lambda}(0)$ and $\widetilde{\widehat{\mu}}(0) = c\,\widehat{\mu}(0)$, then there is a G^2-contact at all points of $\widehat{\mathbf{g}}(0) = \widetilde{\widehat{\mathbf{g}}}(0)$ if and only if $\dot{\tilde{\delta}}(0) = c\,\dot{\delta}(0)$.

Proof: The dual vector function $\widehat{\mathbf{g}}(t)$ determines the real parametrization $\mathbf{x}(t,u)$ of the ruled surface as presented in (14). The partial derivatives at $t = 0$, as given in (16), define the coefficients of the *first fundamental form* as

$$\begin{aligned} E(0,u) &= \mathbf{x}_t \cdot \mathbf{x}_t = \lambda^2 u^2 + \lambda_0^2, \\ F(0,u) &= \mathbf{x}_t \cdot \mathbf{x}_u = 0, \\ G(0,u) &= \mathbf{x}_u \cdot \mathbf{x}_u = 1. \end{aligned} \tag{22}$$

For the coefficients of the *second fundamental form* we obtain

$$\begin{aligned} L &= \frac{1}{\|\mathbf{b}\|}\mathbf{b} \cdot \mathbf{x}_{tt} = \frac{1}{\sqrt{\lambda_0^2 + \lambda^2 u^2}}\Big[\\ &\quad -\lambda_0(\lambda_0\mu + \lambda\mu_0) + (\dot{\lambda}\lambda_0 - \lambda\dot{\lambda}_0)u - \lambda^2\mu u^2\Big], \\ M &= \frac{1}{\|\mathbf{b}\|}\mathbf{b} \cdot \mathbf{x}_{tu} = \frac{1}{\sqrt{\lambda_0^2 + \lambda^2 u^2}}\lambda\lambda_0, \\ N &= \frac{1}{\|\mathbf{b}\|}\mathbf{b} \cdot \mathbf{x}_{uu} = 0. \end{aligned} \tag{23}$$

For the sake of brevity we skip the detailed analysis, which reveals that at any point $\mathbf{x}(0,u)$ on the common generator $t = 0$ the equations $\widetilde{E} = c^2 E$, $\widetilde{L} = c^2 L$, and $\widetilde{M} = cM$ characterize the G^2-contact between the two surfaces. □

5. THE CURVATURE OF THE RULED TOOTH FLANKS

In the realm of gearing, we need two different Frenet frames, the frame $(\widehat{\mathbf{f}}_1, \widehat{\mathbf{f}}_2, \widehat{\mathbf{f}}_3)$ for the axodes with the ISA $\widehat{\mathbf{f}}_1$ (see Fig. 1) and the frame $(\widehat{\mathbf{g}}_1, \widehat{\mathbf{g}}_2, \widehat{\mathbf{g}}_3)$ for conjuate tooth flanks with $\widehat{\mathbf{g}}_1$ as the meshing line (see Fig. 4).

5.1 The Frenet Frame of the Axodes

Upon gear meshing, the *Frenet frame* $(\widehat{\mathbf{f}}_1, \widehat{\mathbf{f}}_2, \widehat{\mathbf{f}}_3)$ of the axodes with $\widehat{\mathbf{f}}_1 = \widehat{\mathbf{p}}_{32}$ remains fixed in the gear frame Σ_1. The second axis $\widehat{\mathbf{f}}_2$ equals the spear $\widehat{\mathbf{e}}_3$ along the common perpendicular of the gear axes $\widehat{\mathbf{p}}_{21}$ and $\widehat{\mathbf{p}}_{31}$. In terms of the basis $(\widehat{\mathbf{e}}_1, \widehat{\mathbf{e}}_2, \widehat{\mathbf{e}}_3)$ we obtain from (3) (see Fig. 1)

$$\begin{pmatrix} \widehat{\mathbf{f}}_1 \\ \widehat{\mathbf{f}}_2 \\ \widehat{\mathbf{f}}_3 \end{pmatrix} = \begin{pmatrix} \cos\widehat{\varphi} & \sin\widehat{\varphi} & 0 \\ 0 & 0 & 1 \\ \sin\widehat{\varphi} & -\cos\widehat{\varphi} & 0 \end{pmatrix} \begin{pmatrix} \widehat{\mathbf{e}}_1 \\ \widehat{\mathbf{e}}_2 \\ \widehat{\mathbf{e}}_3 \end{pmatrix}. \quad (24)$$

The origin of this Frenet frame is the striction point $S = (0, 0, \varphi_0)$ of the axodes, the point of intersection between the ISA $\widehat{\mathbf{p}}_{32}$ and the common normal of $\widehat{\mathbf{p}}_{21}$ and $\widehat{\mathbf{p}}_{31}$. The movement of this frame along the axode $\Pi_2 \subset \Sigma_2$ is the rotation Σ_1/Σ_2 about the axis $\widehat{\mathbf{p}}_{21}$ with the angular velocity $-\omega_{21}$. Therefore

$$\widehat{\mathbf{p}}_{21} = \cos(\widehat{\varphi}+\widehat{\alpha})\widehat{\mathbf{f}}_1 + \sin(\widehat{\varphi}+\widehat{\alpha})\widehat{\mathbf{f}}_3$$

is the permanent Disteli axis of Π_2. Due to (1), the corresponding Frenet equations (note $\widehat{\mathbf{e}}_3 = \widehat{\mathbf{f}}_2$) begin with

$$\begin{aligned} \dot{\widehat{\mathbf{f}}}_1 &= -\omega_{21}\widehat{\mathbf{p}}_{21} \times \widehat{\mathbf{f}}_1 = -\omega_{21}\sin(\widehat{\varphi}+\widehat{\alpha})\widehat{\mathbf{f}}_2 \\ &= -\omega_{21}\left[\sin(\varphi+\alpha) + \varepsilon(\varphi_0+\alpha_0)\cos(\varphi+\alpha)\right]\widehat{\mathbf{f}}_2, \end{aligned}$$

which implies for the axode Π_2 the distribution parameter[4]

$$\delta_2 = (\varphi_0+\alpha_0)\cot(\varphi+\alpha)$$

and the coefficients

$$\widehat{\lambda}_2 = -\omega_{21}\sin(\widehat{\varphi}+\widehat{\alpha}),\ \widehat{\mu}_2 = -\omega_{21}\cos(\widehat{\varphi}+\widehat{\alpha}).$$

[4] For the generators of a one-sheet hyperboloid of revolution with semiaxes a, b the absolute value of the distribution parameter equals the secondary semiaxis, i.e., $|\delta| = b$.

The last equation follows from the third Frenet equation $\dot{\widehat{\mathbf{f}}}_3 = -\omega_{21}\widehat{\mathbf{p}}_{21} \times \widehat{\mathbf{f}}_3$ in (13), and it confirms for the dual angle $\widehat{\gamma}_2$ between the generator $\widehat{\mathbf{p}}_{32} = \widehat{\mathbf{f}}_1$ and the Disteli axis $\widehat{\mathbf{p}}_{21}$ by (21) $\widehat{\gamma}_2 = \widehat{\varphi} + \widehat{\alpha}$ with $\cot\widehat{\gamma}_2 = \widehat{\mu}_2/\widehat{\lambda}_2$ as *dual curvature* of Π_2 according to [1, Theorem 3].

In a similar way we obtain for Π_3 the distribution parameter

$$\delta_3 = (\varphi_0-\alpha_0)\cot(\varphi-\alpha)$$

and the coefficients

$$\widehat{\lambda}_3 = -\omega_{31}\sin(\widehat{\varphi}-\widehat{\alpha}),\ \widehat{\mu}_3 = -\omega_{31}\cos(\widehat{\varphi}-\widehat{\alpha}).$$

The equation $\delta_2 = \delta_3$, which can also be concluded from (5), guarantees the contact between Π_2 and Π_3 at all points of the ISA $\widehat{\mathbf{p}}_{32}$.

In the Frenet equations of the auxiliary surface $\Pi_4 \subset \Sigma_4$ with axis

$$\widehat{\mathbf{p}}_{41} = \cos(\widehat{\varphi}-\widehat{\beta})\widehat{\mathbf{f}}_1 + \sin(\widehat{\varphi}-\widehat{\beta})\widehat{\mathbf{f}}_3$$

and dual velocity $-\widehat{\omega}_{41}$ we obtain the coefficients

$$\begin{aligned} \widehat{\lambda}_4 &= -\widehat{\omega}_{41}\sin(\widehat{\varphi}-\widehat{\beta}), \\ \widehat{\mu}_4 &= -\widehat{\omega}_{41}\cos(\widehat{\varphi}-\widehat{\beta}). \end{aligned} \quad (25)$$

As a consequence, Π_4 has, by virtue of (19), the distribution parameter

$$\delta_4 = h_{41} + (\varphi_0-\beta_0)\cot(\varphi-\beta).$$

The equation $\delta_4 = \delta_3 = \delta_2$ can be verified using Eqs. (4), (9), and (12). The axis of Π_4 makes, with all generators Π_4, the dual angle $\widehat{\gamma}_4 = \widehat{\varphi} - \widehat{\beta}$.

5.2 The Frenet Frame of the Tooth Flanks

According to Theorem 2, any line $\widehat{\mathbf{g}}$ attached to the auxiliary surface Π_4 traces conjugate tooth flanks Φ_2 and Φ_3 under the respective relative motions Σ_4/Σ_2 and Σ_4/Σ_3 with the auxiliary surface Π_4 roll-sliding on the axodes Π_2 and Π_3, respectively. The motion Σ_4/Σ_2 is the composition of Σ_4/Σ_1 with the Frenet motion Σ_1/Σ_2 along Π_2.

We can set up the moving line $\widehat{\mathbf{g}}$ by

$$\widehat{\mathbf{g}} = \cos\widehat{\eta}\,\widehat{\mathbf{f}}_1 + \sin\widehat{\eta}\,\cos\widehat{\xi}\,\widehat{\mathbf{f}}_2 + \sin\widehat{\eta}\,\sin\widehat{\xi}\,\widehat{\mathbf{f}}_3. \tag{26}$$

This follows because the common perpendicular $\widehat{\mathbf{k}}$ between $\widehat{\mathbf{g}}$ and the ISA $\widehat{\mathbf{f}}_1$ (see Fig. 4) can be written as $\mathbf{k} = -\sin\widehat{\xi}\,\widehat{\mathbf{f}}_2 + \cos\widehat{\xi}\,\widehat{\mathbf{f}}_3$. The dual angles $\widehat{\xi}$ and $\pi/2 - \widehat{\eta}$ can be seen as 'dual geographical longitude' and 'latitude', respectively.

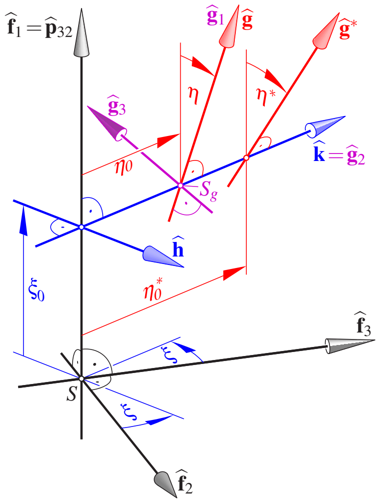

Figure 4: The triplet $(\widehat{\mathbf{g}}_1, \widehat{\mathbf{g}}_2, \widehat{\mathbf{g}}_3)$ is the Frenet frame for the conjugate tooth flanks Φ_2 and Φ_3. The corresponding Disteli axes $\widehat{\mathbf{g}}^*$ are defined by the spatial Euler-Savary equation.

The common perpendicular $\widehat{\mathbf{k}}$ is already the central normal $\widehat{\mathbf{n}}$ of the tooth flanks. This follows because, for the trajectory of $\widehat{\mathbf{g}}$ under Σ_4/Σ_2, we obtain

$$\begin{aligned}\dot{\widehat{\mathbf{g}}} &= \widehat{\omega}_{42}\widehat{\mathbf{f}}_1 \times \widehat{\mathbf{g}} = \widehat{\omega}_{42}\sin\widehat{\eta}\,(\cos\widehat{\xi}\,\widehat{\mathbf{f}}_3 - \sin\widehat{\xi}\,\widehat{\mathbf{f}}_2) \\ &= \widehat{\omega}_{42}\sin\widehat{\eta}\,\widehat{\mathbf{k}}.\end{aligned}$$

Therefore, the Frenet frame $(\widehat{\mathbf{g}}_1 = \widehat{\mathbf{g}},\ \widehat{\mathbf{g}}_2 = \widehat{\mathbf{n}} = \widehat{\mathbf{k}},\ \widehat{\mathbf{g}}_3 = \widehat{\mathbf{t}})$ for the conjugate tooth flanks Φ_2 and Φ_3 has the inital pose

$$\begin{pmatrix}\widehat{\mathbf{g}}_1\\ \widehat{\mathbf{g}}_2\\ \widehat{\mathbf{g}}_3\end{pmatrix} = \widehat{\mathbf{M}}\begin{pmatrix}\widehat{\mathbf{f}}_1\\ \widehat{\mathbf{f}}_2\\ \widehat{\mathbf{f}}_3\end{pmatrix} \text{ with}$$
$$\widehat{\mathbf{M}} = \begin{pmatrix}\cos\widehat{\eta} & \sin\widehat{\eta}\cos\widehat{\xi} & \sin\widehat{\eta}\sin\widehat{\xi}\\ 0 & -\sin\widehat{\xi} & \cos\widehat{\xi}\\ \sin\widehat{\eta} & -\cos\widehat{\eta}\cos\widehat{\xi} & -\cos\widehat{\eta}\sin\widehat{\xi}\end{pmatrix}. \tag{27}$$

From $\dot{\widehat{\mathbf{g}}} = \widehat{\omega}_{42}\widehat{\mathbf{f}}_1 \times \widehat{\mathbf{g}}$ follows by differentiation because of $\widehat{\omega}_{42} = \text{const.}$ the relation below:

$$\ddot{\widehat{\mathbf{g}}} = \widehat{\omega}_{42}\Big[(\dot{\widehat{\mathbf{f}}}_1 \times \widehat{\mathbf{g}}) + (\widehat{\mathbf{f}}_1 \times \dot{\widehat{\mathbf{g}}})\Big].$$

During the motion Σ_4/Σ_2 the ISA $\widehat{\mathbf{f}}_1$ traces Π_2 with angular velocity $-\omega_{21}$. Therefore

$$\dot{\widehat{\mathbf{f}}}_1 = -\omega_{21}\,\widehat{\mathbf{p}}_{21} \times \widehat{\mathbf{f}}_1 = -\omega_{21}\sin(\widehat{\varphi} + \widehat{\alpha})\widehat{\mathbf{f}}_2$$

and hence,

$$\begin{aligned}\ddot{\widehat{\mathbf{g}}} &= \widehat{\omega}_{42}\big[-\omega_{21}\sin(\widehat{\varphi}+\widehat{\alpha})(\widehat{\mathbf{f}}_2 \times \widehat{\mathbf{g}}) \\ &\qquad + \widehat{\mathbf{f}}_1 \times \widehat{\omega}_{42}(\widehat{\mathbf{f}}_1 \times \widehat{\mathbf{g}})\big] \\ &= \widehat{\omega}_{42}\big[-\omega_{21}\sin(\widehat{\varphi}+\widehat{\alpha})(\widehat{\mathbf{f}}_2 \times \widehat{\mathbf{g}}) \\ &\qquad + \widehat{\omega}_{42}\big((\widehat{\mathbf{f}}_1 \cdot \widehat{\mathbf{g}})\widehat{\mathbf{f}}_1 - (\widehat{\mathbf{f}}_1 \cdot \widehat{\mathbf{f}}_1)\widehat{\mathbf{g}}\big)\big].\end{aligned}$$

By (27), we can express the first and second derivatives of $\widehat{\mathbf{g}}$ in the Frenet frame $(\widehat{\mathbf{g}}_1, \widehat{\mathbf{g}}_2, \widehat{\mathbf{g}}_3)$ as

$$\begin{aligned}\dot{\widehat{\mathbf{g}}} &= \dot{\widehat{\mathbf{g}}}_1 = \widehat{\omega}_{42}\widehat{\mathbf{f}}_1 \times \widehat{\mathbf{g}} = \widehat{\omega}_{42}\sin\widehat{\eta}\,\widehat{\mathbf{g}}_2,\\ \ddot{\widehat{\mathbf{g}}} &= \widehat{\omega}_{42}\big[\widehat{\omega}_{42}\sin^2\widehat{\eta}\,\widehat{\mathbf{g}}_1 \\ &\quad + \omega_{21}\sin(\widehat{\varphi}+\widehat{\alpha})\cos\widehat{\xi}\cos\widehat{\eta}\,\widehat{\mathbf{g}}_2 \\ &\quad + \big(-\omega_{21}\sin(\widehat{\varphi}+\widehat{\alpha})\sin\widehat{\xi} + \widehat{\omega}_{42}\sin\widehat{\eta}\cos\widehat{\eta}\big)\widehat{\mathbf{g}}_3\big],\end{aligned}$$

which, upon comparison with (15), yields the instantanous invariants of the tooth flank Φ_2 under $\eta \neq 0$, i.e., $\widehat{\mathbf{g}}$ not parallel to the ISA $\widehat{\mathbf{f}}_1$, as

$$\begin{aligned}\widehat{\lambda}_{\Phi_2} &= \widehat{\omega}_{42}\sin\widehat{\eta},\\ \widehat{\mu}_{\Phi_2} &= -\omega_{21}\frac{\sin(\widehat{\varphi}+\widehat{\alpha})\sin\widehat{\xi}}{\sin\widehat{\eta}} + \widehat{\omega}_{42}\cos\widehat{\eta}.\end{aligned} \tag{28}$$

For the conjugate tooth flank Φ_3 we obtain likewise

$$\begin{aligned}\widehat{\lambda}_{\Phi_3} &= \widehat{\omega}_{43}\sin\widehat{\eta},\\ \widehat{\mu}_{\Phi_3} &= -\omega_{31}\frac{\sin(\widehat{\varphi}-\widehat{\alpha})\sin\widehat{\xi}}{\sin\widehat{\eta}} + \widehat{\omega}_{43}\cos\widehat{\eta}.\end{aligned} \tag{29}$$

When the dual angle $\widehat{\eta}^*_{\Phi_i}$ characterizes the instant Disteli axis of Φ_i we can verify the spatial Euler-Savary equation (see [1])

$$\begin{aligned}(\cot\widehat{\eta}^*_{\Phi_2} - \cot\widehat{\eta}\,)\sin\widehat{\xi} &= \cot\widehat{\gamma}_2 - \cot\widehat{\gamma}_4 \\ &= \cot(\widehat{\varphi}+\widehat{\alpha}) - \cot(\widehat{\varphi}-\widehat{\beta})\end{aligned} \tag{30}$$

for the motion Σ_4/Σ_2, which generates Φ_2.

In the same way we can confirm that the Disteli axis $\widehat{\mathbf{g}}^*_{\Phi_3}$ of Φ_3 satisfies

$$\begin{aligned}(\cot\widehat{\eta}^*_{\Phi_3} - \cot\widehat{\eta}\,)\sin\widehat{\xi} &= \cot\widehat{\gamma}_3 - \cot\widehat{\gamma}_4 \\ &= \cot(\widehat{\varphi}-\widehat{\alpha}) - \cot(\widehat{\varphi}-\widehat{\beta}).\end{aligned}$$

Upon subtraction of the two Euler-Savary equations we obtain

$$(\cot\widehat{\eta}^*_{\Phi_2} - \cot\widehat{\eta}^*_{\Phi_3})\sin\widehat{\xi} = \cot\widehat{\gamma}_2 - \cot\widehat{\gamma}_3\,,$$

thereby proving the spatial version of a result which is well known in planar and spherical kinematics, namely

Theorem 5. *Let Φ_2 and Φ_3 be conjugate ruled tooth flanks with permanent line contact. Then the Disteli axes $\widehat{\mathbf{g}}^*_{\Phi_2}$ and $\widehat{\mathbf{g}}^*_{\Phi_3}$ of the instant meshing line satisfy the Euler-Savary equation for the relative motion Σ_3/Σ_2 between the two gears.*

6. A SPATIAL ANALOGUE OF INVOLUTE GEARING

In planar cycloid gearing there are two auxiliary curves, namely two circles, which usually are laid out in a symmetric relative position with respect to the pole tangent. The same is true on the sphere. However, when the auxiliary circles are specified as great circles they become identical, coinciding with the spherical pole tangent t. The axis $\widehat{\mathbf{p}}_{41}$ of the great circle t is orthogonal to the ISA $\widehat{\mathbf{p}}_{32}$. The corresponding profiles are involutes of the polodes; they are characterized by the constant pressure angle $\alpha = 0°$.

This is the particular case of involute gearing where the pitch circles coincide with the base circles. These profiles are **not** geometrically feasable because of one reason: At the meshing point P on the instant pole tangent t the profiles have either

- a G^2-contact with mutual penetration, or
- a cusp, and at external gears the curves open towards opposite sides.

We obtain the corresponding spatial version when we specify the axis $\widehat{\mathbf{p}}_{41}$ orthogonal to the ISA $\widehat{\mathbf{p}}_{32}$ on the Plücker conoid (see Fig. 1). This is the case we analyze below.

Due to Eqs. (4)–(9), the representation $\widehat{\mathbf{p}}_{41} = -\sin\widehat{\beta}\,\widehat{\mathbf{e}}_1 + \cos\widehat{\beta}\,\widehat{\mathbf{e}}_2$ implies

$$\begin{aligned}\beta = \varphi + \frac{\pi}{2}\,,^{5} \quad \beta_0 = -\varphi_0\,,\\ \widehat{\varphi} - \widehat{\beta} = -\frac{\pi}{2} + 2\varepsilon\varphi_0\,.\end{aligned} \tag{31}$$

Therefore,

$$\sin(\widehat{\varphi}-\widehat{\beta}) = -1,\ \cos(\widehat{\varphi}-\widehat{\beta}) = 2\varepsilon\varphi_0\,. \tag{32}$$

From Eqs. (10), (5), and (12) follows for our particular choice

$$\begin{aligned}\widehat{\omega}_{41} &= -\omega_{21}\sin(\widehat{\varphi}+\widehat{\alpha})\\ h_{41} &= R(\cos 2\alpha + \cos 2\varphi).\end{aligned} \tag{33}$$

The auxiliary surface Π_4 is a skew orthogonal helicoid with axis $\widehat{\mathbf{p}}_{41}$ and pitch h_{41}, the ISA $\widehat{\mathbf{p}}_{32}$ being its initial generator. The invariants of Π_4 are, by virtue of (25),

$$\widehat{\lambda}_4 = \widehat{\omega}_{41}\,, \quad \widehat{\mu}_4 = -2\varepsilon\varphi_0\,\widehat{\omega}_{41}\,. \tag{34}$$

The dual angle between the generators of Π_4 and its axis is

$$\begin{aligned}\widehat{\gamma}_4 = \widehat{\varphi} - \widehat{\beta} = -\frac{\pi}{2} + 2\varepsilon\varphi_0 \ \text{with}\\ \cot\widehat{\gamma}_4 = \widehat{\mu}_4/\widehat{\lambda}_4 = -2\varepsilon\varphi_0\,.\end{aligned}$$

From (4), the distance γ_{40} between axis and generators vanishes if and only if $\varphi = 0$, i.e., $\omega_{21} = -\omega_{31}$.

The generating motions Σ_4/Σ_2 and Σ_4/Σ_3 of the tooth flanks Φ_2 and Φ_3 have the twists $\widehat{\mathbf{q}}_{42} =$

[5] One could also set $\beta = \varphi - \pi/2$. However, this has no effect on the auxiliary surface. It only reverses the orientation of $\widehat{\mathbf{p}}_{41}$ and changes therefore the sign of ω_{41} and ω_{410}.

$\widehat{\omega}_{42}\widehat{\mathbf{f}}_1$ and $\widehat{\mathbf{q}}_{43} = \widehat{\omega}_{43}\widehat{\mathbf{f}}_1$, respectively; in our particular case we have

$$\begin{aligned}\widehat{\omega}_{42} &= -\omega_{21}\,[\cos(\varphi+\alpha)+\varepsilon(\varphi_0-\alpha_0)\sin(\varphi+\alpha)]\,,\\ \widehat{\omega}_{43} &= -\omega_{31}\,[\cos(\varphi-\alpha)+\varepsilon(\varphi_0+\alpha_0)\sin(\varphi-\alpha)]\,.\end{aligned} \tag{35}$$

Hence,

$$\begin{aligned}\widehat{\omega}_{43}:\widehat{\omega}_{42} &= \tan(\varphi+\alpha):\tan(\varphi-\alpha)\\ &= (\varphi_0+\alpha_0):(\varphi_0-\alpha_0).\end{aligned} \tag{36}$$

6.1 The ISA as a Line of Regression

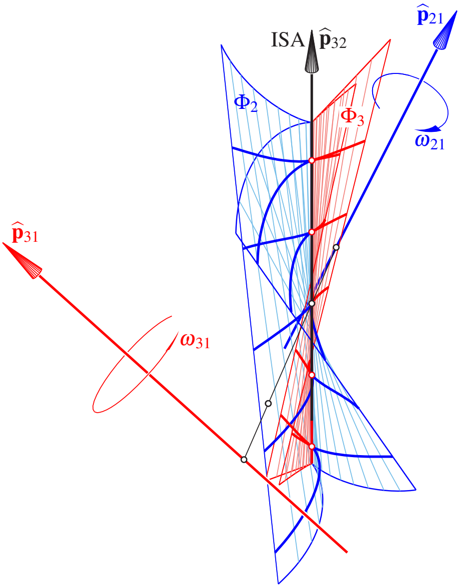

Figure 5: When the ISA coincides with the meshing line $\widehat{\mathbf{g}}$, the singular lines of the two flanks Φ_2, Φ_3 come together sharing the tangent plane at each point of $\widehat{\mathbf{g}}$; but the flanks open toward opposite sides. The fat red and blue lines indicate sections orthogonal to the ISA.

Analogue to the planar and spherical cases, in spatial cycloid gearing the ISA $\widehat{\mathbf{p}}_{32}$ is a singular generator of the two tooth flanks Φ_2 and Φ_3. As pointed out in [6, Theorem 5], all its points are uniplanar, the tangent planes along $\widehat{\mathbf{p}}_{32}$ being distributed just as along a regular generator with distribution parameter $\delta = R\cos 2\alpha$. Figure 8 in [6] reveals that the ISA doesn't look singular at all; it is the common border line of the two components, orginating from two symmetrically placed auxiliary surfaces. However, in our particular case the two auxiliary surfaces coincide with the skew helicoid Π_4. The ISA is, in fact, a line of regression for both tooth flanks. In external gears, as depicted in Fig. 5, the two flanks open toward opposite sides. Hence, when the ISA becomes the meshing line, no transmission of forces can take place. Figure 5 shows the conjugate tooth flanks as wire-frames; the depicted fat red and blue lines being the intersections of the flanks with planes perpendicular to the ISA.

6.2 There is a G^2-contact at the Striction Point

What corresponds in skew gears to the osculation of tooth profiles when the pole tangent serves as auxiliary curve ?

Figure 6 shows an example[6] where the initial meshing line $\widehat{\mathbf{g}}$ differs from the ISA. But $\widehat{\mathbf{g}}$ is parallel to the ISA and intersects the central tangent of the axodes at right angles. This central tangent passes through the striction point S of the axodes and is parallel to the axis $\widehat{\mathbf{p}}_{41}$ of the auxiliary surface Π_4 (note $\widehat{\mathbf{f}}_3$ in Fig. 1).

The spatial Euler-Savary equation (30) (see [1, Theorem 6]) for the motion Σ_4/Σ_2

$$(\cot\widehat{\eta}^* - \cot\widehat{\eta})\sin\widehat{\xi} = \frac{\widehat{\omega}}{\widehat{\lambda}} = \cot\widehat{\gamma}_2 - \cot\widehat{\gamma}_4,$$

holds only under $\sin\widehat{\xi} \neq 0$, but we can replace it by the equation [1, page 13]

$$\begin{aligned}\widehat{\lambda}\,\sin\widehat{\xi}\,(\cos\widehat{\eta}\,\sin\widehat{\eta}^* - \sin\widehat{\eta}\,\cos\widehat{\eta}^*)&\\ +\widehat{\omega}\,\sin\widehat{\eta}\,\sin\widehat{\eta}^* = 0\,.&\end{aligned}$$

Under the relation $\sin\widehat{\xi} = 0$ (i.e., $\widehat{\mathbf{k}} = \widehat{\mathbf{f}}_3$ in Fig. 4) it is apparent that $\sin\widehat{\eta} \neq 0$ implies $\sin\widehat{\eta}^* = 0$. In other words, when $\widehat{\mathbf{g}} \neq \widehat{\mathbf{p}}_{32}$ intersects the striction tangent $\widehat{\mathbf{f}}_3$ of the axodes at right angles, the

[6] Data: $2\alpha = 60.0°$, $2\alpha_0 = 70.0\,\mathrm{mm}$, $\omega_{31}:\omega_{21} = -2:3$, and distance between the ISA and the initial meshing line $\widehat{\mathbf{g}}$: $\overline{SS_g} = 35.0\,\mathrm{mm}$.

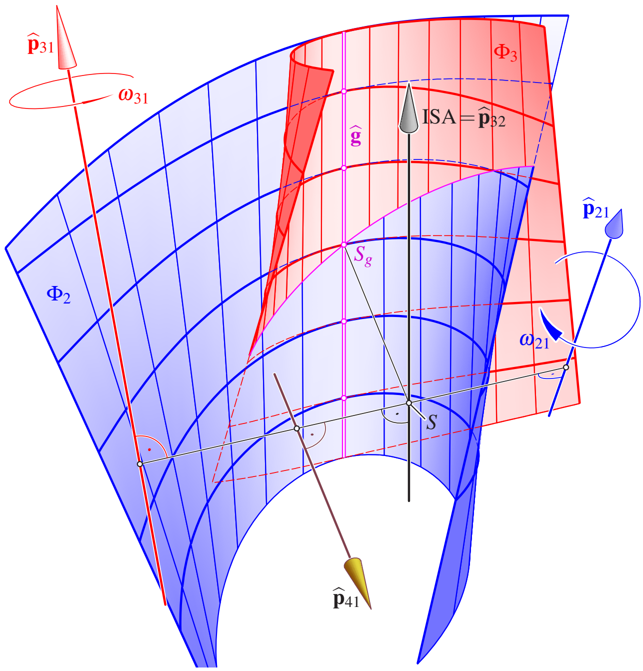

Figure 6: Two conjugate flanks Φ_2 and Φ_3 with G^2 -contact at the common striction point S_g. The meshing line $\widehat{\mathbf{g}}$ is parallel to the ISA and a cylindric generator of Φ_2 and Φ_3.

Disteli axis $\widehat{\mathbf{g}}^*$ coincides with the ISA. The same holds for the motion Σ_4/Σ_3, which means that under this condition the two tooth flanks share the instant Disteli axis. According to Theorem 4, Φ_2 and Φ_3 have a G^2-contact at the common striction point S_g.

In Fig. 6, the fat blue and read curves, which are in contact at marked points on the meshing line $\widehat{\mathbf{g}}$, are level lines of the two flanks, i.e., intersections with planes orthogonal to the ISA. The mean section shows the G^2-contact at the striction point S_g, which causes the penetration.

The case of osculating cylindrical or spherical tooth flanks is misleading. In the true spatial version there is no G^2-contact at all other points of $\widehat{\mathbf{g}}$ for one reason: According to Theorem 4, in this case the condition $\dot{\tilde{\delta}}(0) = c\,\dot{\delta}(0)$ must be satisfied. However, because of the permanent line contact the flanks have the same distribution parameter $\tilde{\delta}(t) = \delta(t)$ for each $t \in I$. This implies $\dot{\tilde{\delta}}(0) = \dot{\delta}(0)$, but by Eqs. (28), (29) and (36), the constant c with $\widehat{\lambda}_{\Phi_3} = c\,\widehat{\lambda}_{\Phi_2}$ is

$$\begin{aligned} c &= \tan(\varphi+\alpha)/\tan(\varphi-\alpha) \\ &= (\varphi_0+\alpha_0):(\varphi_0-\alpha_0) \neq 1. \end{aligned}$$

The different poses depicted in Fig. 7 reveal that there is also a mutual penetration of the conjugate tooth flanks Φ_2 and Φ_3 at the other poses. Since the surfaces share this curve of intersection as well as the tangent planes at all points of the meshing line, there must be a G^2-contact at the point where the curve of intersection meets the meshing line. This point is close to the mar-

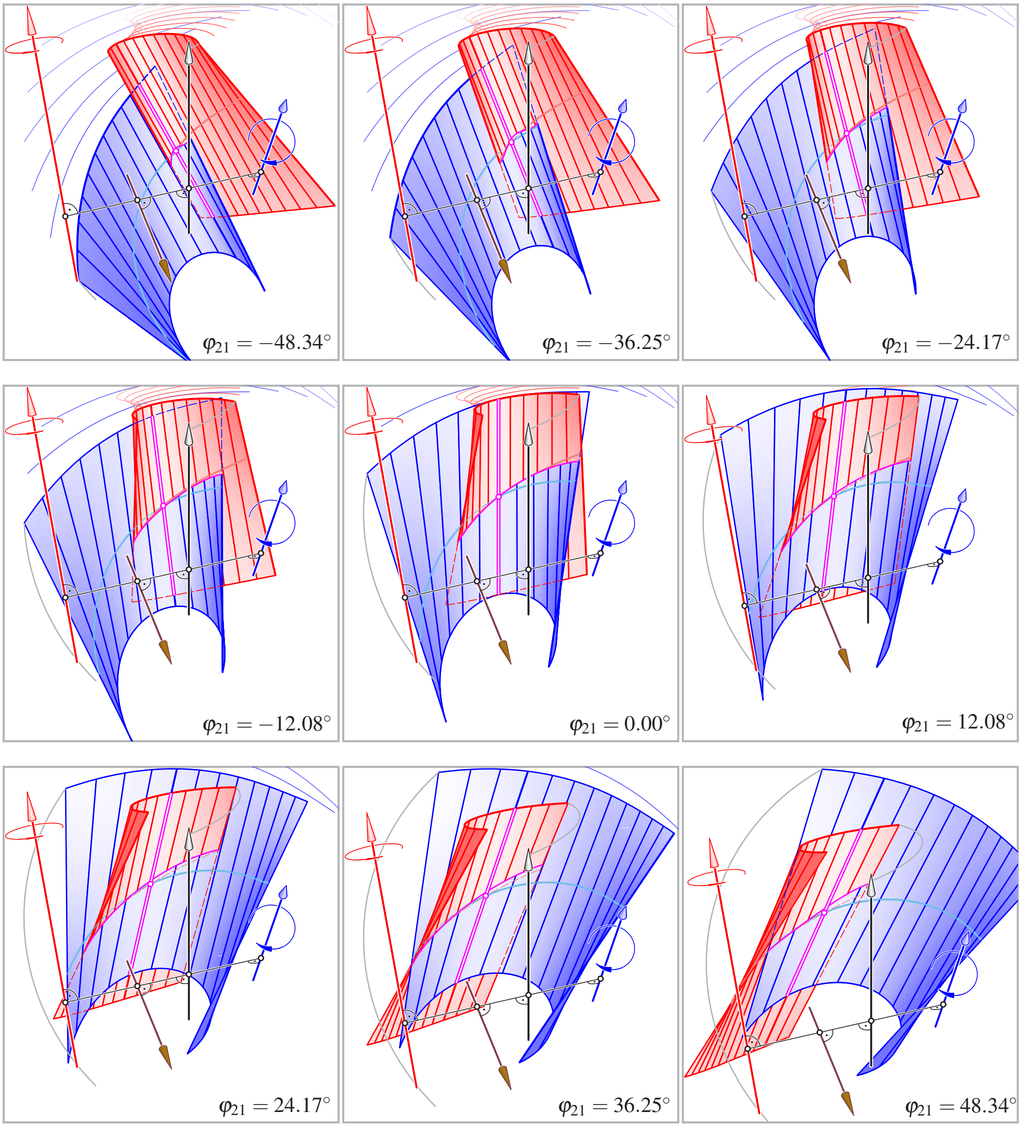

Figure 7: Snapshots of the penetrating tooth flanks with their striction curves upon meshing.

ked striction point; however it can be proved that the point of G^2-contact must be different from the striction point S_g up to the symmetric case $\omega_{31} = -\omega_{21}$; hence $\varphi_0 = 0$.

6.3 A Spatial Analogue of Octoidal Gears

In the plane as well as on the sphere, the *generalized Camus Theorem* states that for any curve c_4 attached to the auxiliary curve $p_4 \subset \Sigma_4$ the envelopes c_2 and c_3 under motions Σ_4/Σ_2 and Σ_4/Σ_3, respectively, are conjugate tooth profiles.

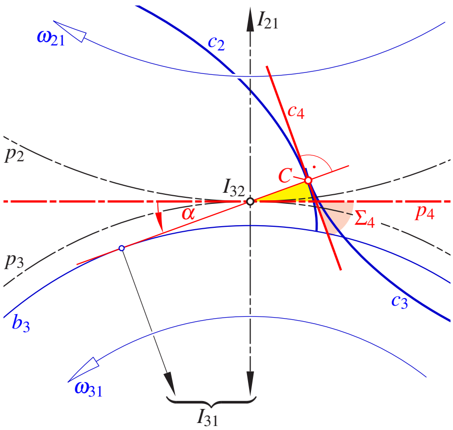

Figure 8: Planar version of the generalized Camus Theorem in the particular case leading to involute gears.

In the particular planar case, depicted in Fig. 8, the auxiliary curve p_4 is the pole tangent t and the attached curve c_4 is a line. In all its poses, the line c_4 shows the same inclination with respect to the gear frame Σ_1. At each pose, the enveloping point C of c_4 is the pedal point with respect to the instant pole I_{32}. The right-angled triangle enclosed by c_4, p_4 and the line $I_{32}C$ shows that the pressure angle α remains constant, which leads to the case of involute gearing.

The foregoing statement does not hold in spherical geometry since for spherical triangles the sum of the interior angles is not constant. This sum is always greater than 180°, the amount

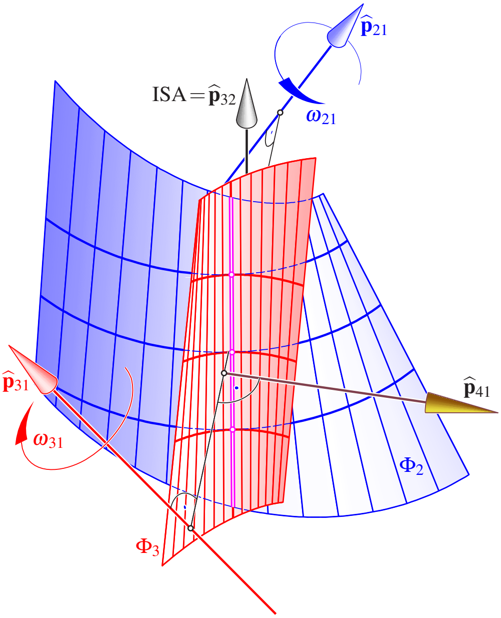

Figure 9: Skew gears with torses as conjugate tooth flanks Φ_2, Φ_3 and permanent line contact. The fat red and blue lines indicate sections orthogonal to the meshing line.

by which the sum exceeds 180° being proportional to the area of the triangle. Therefore, we cannot conclude for the analog specification in bevel gears that the pressure angle α is constant; it increases with the distance between I_{32} and c_4. We obtain what is known as *octoidal gears*, as reported in [3].

The validity of the spatial analogue of the generalized Camus Theorem was proved in [6, Theorem 6]: For any surface Φ_4 attached to the auxiliary surface Π_4 the envelopes Φ_2 and Φ_3 under the respective relative motions Σ_4/Σ_2 and Σ_4/Σ_3 are conjugate tooth flanks. We choose again Π_4 as the skew orthogonal helicoid and specify Φ_4 as a plane. Then we obtain a pair of conjugate torses Φ_2, Φ_3 with permanent line contact. In Fig. 9 one example is depicted which indicates

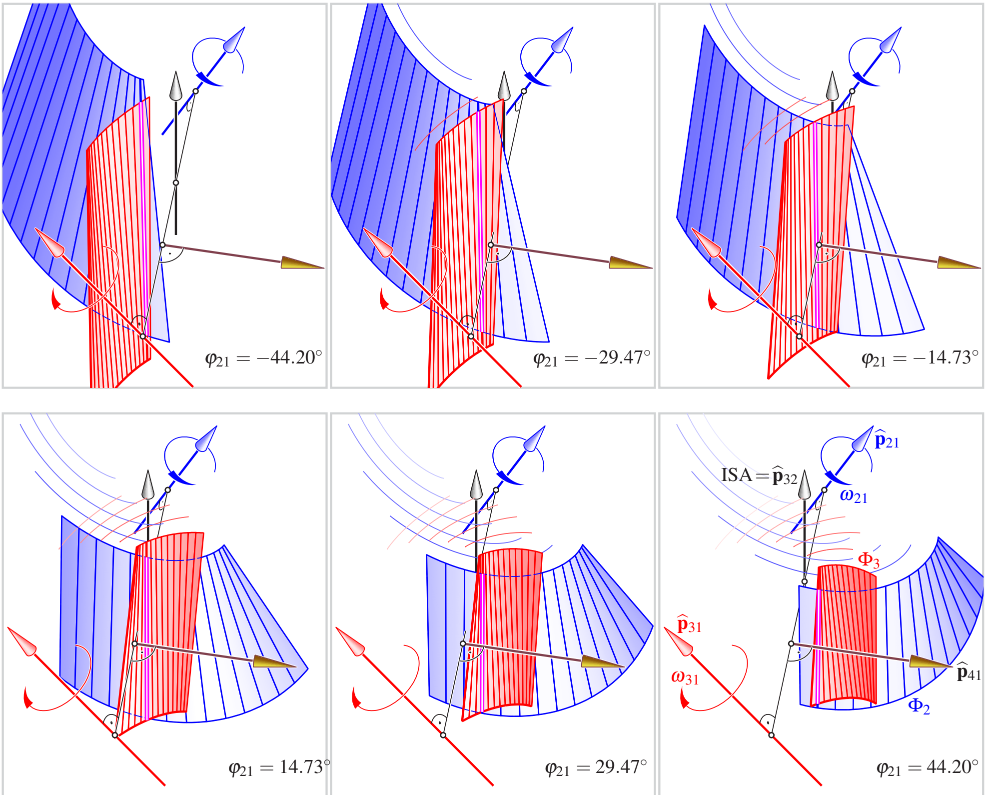

Figure 10: Snapshots of the conjugate torses Φ_2 and Φ_3 upon meshing $(\omega_{31} : \omega_{21} = -2 : 1)$.

that these flanks should work correctly. Contrary to the general case of J. Phillips' involute gearing [7], contact is not punctual, but along a line.

The fat red an blue curves in Fig. 9 are the intersections of the flanks with planes perpendicular to the instant meshing line, which is depicted as magenta double line. Figure 10 shows snapshots of the conjugate torses upon meshing.

7. CONCLUSIONS

Based on the Camus Theorem and on Martin Disteli's work, we showed in this paper that the flanks of spatial cycloid gears can be synthesized by means of an auxiliary surface. Upon choosing the skew orthogonal helicoid as auxiliary surface, the tooth flanks of the spatial equivalent of octoidal gears are obtained. The final example with torses as conjugate tooth flanks looks promising but still needs a detailed analysis.

REFERENCES

[1] Stachel, H. (2000). Instantaneous spatial kinematics and the invariants of the axodes, *Proc. Ball 2000 Symposium*, Cambridge (article no. 23).

[2] Blaschke, W. (1960). *Kinematik und Quaternionen,* VEB Deutscher Verlag der Wissenschaften, Berlin.